NEUTRON DETECTION UTILIZING GADOLINIUM DOPED HAFNIUM OXIDE FILMS

THESIS

Bryan D. Blasy, 2Lt, USAF

AFIT/GNE/ENP/08-M02

DEPARTMENT OF THE AIR FORCE
AIR UNIVERSITY

AIR FORCE INSTITUTE OF TECHNOLOGY

Wright-Patterson Air Force Base, Ohio

The views expressed in this thesis are those of the author and do not reflect the official policy or position of the United States Air Force, Department of Defense, or the United States Government.

AFIT/GNE/ENP/08-M02

NEUTRON DETECTION UTILIZING GADOLINIUM DOPED HAFNIUM OXIDE FILMS

THESIS

Presented to the Faculty

Department of Engineering Physics

Graduate School of Engineering and Management

Air Force Institute of Technology

Air University

Air Education and Training Command

In Partial Fulfillment of the Requirements for the

Degree of Master of Science in Nuclear Engineering

Bryan D. Blasy

2Lt, USAF

March 2008

AFIT/GNE/ENP/08-M02

NEUTRON DETECTION UTILIZING GADOLINIUM DOPED HAFNIUM OXIDE FILMS

Bryan D. Blasy, BS
2Lt, USAF

Approved:

_____//Signed//_____	25 Mar 08
David A. LaGraffe (Chairman)	date
_____ //Signed//_____	25 Mar 08
James C. Petrosky (Member)	date
_____//Signed//_____	25 Mar 08
Ronald F. Tuttle (Member)	date

Abstract

Gadolinium (Gd) doped hafnium oxide (HfO_2) was deposited onto a silicon substrate using pulsed laser deposition. Synchrotron radiation was used to perform Gd L3-edge extended X-ray absorption fine structure (EXAFS) measurements on 3%, 10%, and 15% doped HfO_2 samples. The interatomic distances determined from Fourier transformation and fitting the data show Gd occupying the hafnium site in the HfO_2 lattice, there was no clustering of Gd atoms, and the Gd ion retains monoclinic local symmetery for all levels of doping. Current as a function of voltage experiments identified the films as having poor diode characteristics with high leakage current in the forward bias region. However, a proper bias (0.5 V) for the purpose of neutron detection was identified and applied across the diodes. Using a high, non-varying neutron flux in a nuclear reactor, Gd doped HfO_2 was able to be used in a detection system and displayed the ability to detect neutrons.

Acknowledgments

Although this project was supposed to be mainly self directed, I personally could not have completed it without assistance from many professors, colleagues, family and friends. I sincerely thank the following people and hope I can return the favors.

The first person that deserves my thanks is LTC David LaGraffe. His guidance has not only pointed me in the right direction and kept me from making mistakes (of which I am prone), but also made this project and subject matter interesting and somewhat comical. These things are a must keep me on task, and I could not have asked for a better guide.

My thesis committee, Dr. James Petrosky, and Dr. Ronald Tuttle, whose grilling during my prospectus defense made me ensure I was prepared to defend myself against a barrage of PhD questions. What a humbling experience! I thank them for their time and effort in helping me finish my project.

I gathered my data and samples from three different universities. The first was the University of Nebraska-Lincoln. There Dr. Peter Dowben and his group were a large help in me obtaining samples and learning how they were made. He also, to my amazement, found the kindness to include me in some published papers. The Lousiana State University CAMD staff, where I obtained my data from the synchrotron was also extremely helpful in aiding me when I was first learning about this subject. Yuroslav and Alex, I thank you for your data interpretation skills and for taking me out for drinks. The last place was The Ohio State University Research Reactor. Here, I spent most of my data collection time and required the assistance both Joseph Talnagi and Andrew

Kauffman. I thank them for their scientific knowledge and keeping cool with my lack of scheduling skills.

Finally, I would like to thank my classmates, friends, and family. My classmates were always around to listen, have a drink with to forget about school for a few hours, and to take my comments about choosing the right branch of service. My friends for doing much of the same, but also for inspiring me to leave the Dayton area for some much needed R&R. You know who you are. Most importantly, I'd like to thank my family. Mom, you love to listen to me complain which is a skill not many can master. Much love and thanks.

Bryan D. Blasy

Table of Contents

Page

Abstract v

Acknowledgments vi

Table of Contents viii

List of Figures x

List of Tables xii

1. Introduction 1-1

1.1. Motivation 1-1
1.2. Background 1-3
1.3. Problem Statement 1-5
1.4. Research Methodology 1-5
1.5. Preview 1-7

2. Theory 2-1

2.1. Energy bands 2-1
2.2. Charge Carriers 2-2
2.3. Dopants and Impurities 2-4
2.4. p-n and Heterojunction Diodes 2-6
2.5. Radiation Detection with Semiconductors 2-8
2.6. Neutron Interaction with Gadolinium 2-9
2.7. Extended X-Ray Absorption Fine Structure (EXAFS) 2-11

3. Experimental Procedures 3-1

3.1. Pulsed Laser Deposition 3-1
3.2. Extended X-Ray Absorption Fine Structure (EXAFS) 3-2
3.3. Current Voltage Temperature Experiments 3-3
3.4. Construction of the Sample Holder 3-5
3.5. Flux Measurements 3-7
3.6. Detection System Set Up and Neutron Detection Experiments 3-9

4. Results and Analysis 4-1

4.1. Extended X-Ray Absorption Fine Structure (EXAFS) 4-1

4.2. Current Voltage Temperature Experiments 4-2
4.3. Flux Measurements 4-5
4.4. Neutron Detection Experiments 4-6

5. Conclusions and Recommendations 5-1

6. Bibliography 6-1

List of Figures

Page

Figure 1-1. Typical detection set-up 1-6

Figure 2-1. Bandgap energies in an insulator and semiconductor 2-1

Figure 2-2. New donor levels created with phosphorus in silicon 2-5

Figure 2-3. Acceptor levels from doping silicon with boron 2-6

Figure 2-4. A p-n junction 2-7

Figure 2-5. Current-voltage characteristics of a typical silicon p-n junction 2-8

Figure 3-1. Pulsed laser deposition 3-2

Figure 3-2. Louisiana State University CAMD facility 3-3

Figure 3-3. CAMD beamline 3-3

Figure 3-4. Equipment set up 3-4

Figure 3-5. Sample holder design 3-6

Figure 3-6. Experiment configuration 3-7

Figure 3-7. Sample holder on polyethylene plug 3-8

Figure 3-8. Beam port 1 3-8

Figure 3-9. Equipment set up 3-10

Figure 4-1. Fourier transform plot 4-2

Figure 4-2. Current vs voltage for old sample 4-3

Figure 4-3. Current vs voltage for new sample set 4-3

Figure 4-4. Current vs voltage temperature dependence 4-5

Figure 4-5. OSU flux spectra 4-6

Figure 4-6. Background and pump noise 4-7

Figure 4-7. Neutron spectra power comparison 4-9

Figure 4-8. 125 kW neutron spectrum 4-10

Figure 4-9. 250 kW neutron spectrum 4-11

Figure 4-10. 450 kW neutron spectrum 4-12

List of Tables

Page

Table 3-1. TIV equipment 3-4

Table 3-2. Neutron detection equipment 3-9

Neutron Detection Utilizing Gadolinium Doped Hafnium Oxide Films

1. Introduction

The contents of this thesis include the results of a series of experiments involving gadolinium (Gd) doped hafnium oxide (HfO_2) films. These experiments were intended to determine the properties of the films and to determine if this material could be used to detect neutrons in a reactor. The first experiment was an extended X-ray absorption Fine Structure (EXAFS) experiment performed utilizing a synchrotron located at Louisiana State University's Center for Advanced Microstructures and Devices (CAMD) facility. This experiment provided the location of the Gd atoms in the HfO_2 films. The second set was a series of current-voltage (IV) experiments while varying temperature. This provided information on the temperature dependence of the IV curves in the samples, leakage current values, and to determine the optimal applied voltage for neutron detection. The final experiment at The Ohio State University Research Reactor (OSURR) was used to provide a known variable flux to a sample such that neutron pulse counting could be measured.

1.1. Motivation

Approximately 435 reactors are in operation worldwide currently producing ~16% of the world's electricity. The United States produces the most in terms of wattage and France obtains the highest percentage of energy from nuclear power at 80%.

Neutron induced fission is the source of energy in all nuclear reactors. The rate at which this occurs must be monitored for accurate power production, safety, and regulatory concerns. Other than reactors, neutron producing materials are widely used for research, industrial purposes, and nuclear weapons production. Extensive use of these materials also results in safety concerns. Therefore, detection of neutron production is of utmost importance throughout the nuclear community.

The mission of the Defense Threat Reduction Agency (DTRA) is to safeguard America and its allies from Weapons of Mass Destruction (chemical, biological, radiological, nuclear, and high yield explosives) by providing capabilities to reduce eliminate, and counter the threat, and mitigate its effects. Instrumentation with the ability to detect special nuclear material (SNM), uranium-235/233 and plutonium-239, is a necessary asset for the radiological and nuclear missions of DTRA(consisting mainly of deterrence and treaty monitoring). Research and development of new, more efficient neutron detectors is ongoing and appropriately funded by DTRA.[1]

Uranium and plutonium emit low energy gamma rays, alpha particles, and neutron radiation. Many instruments capable of gamma detection have been available for decades. However, most low energy gammas emitted are unlikely to escape weapon components, packaging, or shipping materials at the same emission energy for appropriate detection. Also, many other radionuclides emit gamma rays. This could lead to an assumption that a container contains SNM (false positives). A similar problem exists for alpha radiation. An alpha particle with a large linear energy transfer (LET) cannot travel further than approximately 1/8” in air. Since, background neutron radiation is exceptionally low; the presence of such particles would be a strong indicator of SNM.

1.2. Background

Several methods of neutron detection exist. Virtually all of these methods involve neutrons interacting with a target material to produce charged particles (alpha particles, protons, electrons, etc). It is the subsequent detection of these charged particles in a detection system that provides the evidence of a neutron interaction. This method of interaction is used in systems called active detectors. The word "active" signifies that a pulse or current signal is produced for each neutron interaction. Active neutron detection is currently possible using many different detector systems to include proportional counters, fission chambers, bonner spheres, and semiconductor materials.

Semiconductor detectors, typically called semiconductor diode detectors or just solid state detectors, have been in use since the early 1960s. A solid medium is of great advantage to liquid or gas for the detection of high energy electromagnetic radiation because its density is typically 3 orders of magnitude greater.[2] This allows the same detection efficiency in a smaller medium.

Scintillation detectors are another system utilizing solid medium for radiation detection. Although these detectors are very efficient, they have poor energy resolution. Such detectors convert incident radiation into light for collection and generation into an electric signal for identification in an electronics package. This process requires on the order of 100 eV to produce on electrical signal (called a charge carrier or photoelectron). The number of charge carriers per ionization event is only a few thousand (a very low number). The statistical fluctuations in a few thousand result in poor resolution which is approximately 6% for 662 keV gamma rays. The only method of increasing the statistical limit is to increase the charge carrier production per ionization event in the

material. Semiconductor materials are proven to have the highest charge carrier production of all detector types. Other strengths include compact size, relatively fast timing characteristics, and an effective thickness that can be varied to match the requirements of the application.[2]

Several important factors must be taken into account for proper detection of neutrons. The probability of interaction of a neutron in a material is related to its neutron cross section. Neutron cross sections are material, interaction type (i.e. absorption or scatter), and energy dependent. For purposes of this study, only neutrons below the cadmium cutoff energy (~0.5 eV) will be considered. These are referred to as slow neutrons. Most detection systems utilize the absorption (or capture) reaction mechanism in materials. These reactions are typically neutron to alpha (n,α), neutron to gamma (n,γ), neutron to proton (n,p), etc. Of particular interest here is the (n,γ) reaction, but more specifically its competing process of internal conversion. When the neutron is captured by a nucleus, a majority of the compound nuclei will decay by gamma emission. However, a known percentage will stabilize by emission of an electron. These electrons are of importance in Gd-based solid state detection systems.

Boron has been integrated into neutron detection media for several years. The properties of gadolinium (Gd) have been known for some time, but recently it has been doped onto a semiconducting material for study. Utilization of boron for neutron detection has proven useful. However, a gadolinium-based semiconductor diode detector may prove more useful. The most obvious reason is the extremely large thermal absorption cross section of 255,000 barns in ^{157}Gd as compared to 3840 barns in ^{10}B.[3] The natural isotopic abundance of ^{157}Gd is only 15.65%, but the overall average

absorption cross section of Gd approximately 46,000 barns.[3] Since all neutrons are born at fast energies (on order of MeV), significant moderation is required for a high probability of capture reactions to occur. The Gd cross section extends into energies up to 200 meV, whereas boron requires neutron energy moderation to 25-30 meV.[4] Production of conversion electrons is required for the detection process in Gd, so a high conversion coefficient is important. Fortunately, the conversion coefficient of gadolinium is as high as 30%.[5]

Gadolinium doping of hafnium oxide is a relatively new process. A heterojunction created between Gd and silicon has excellent diode characteristics. For it to be a viable option for neutron detection or other uses, material properties must be experimentally determined. Ensuring the HfO_2 was properly doped with Gd and determining operating voltage for neutron detection are paramount in this experiment.

1.3. Problem Statement

Are gadolinium doped hafnium oxide films useful in a neutron detection system?

1.4. Research Methodology

Determining the effectiveness of a neutron detection system requires a stable and known neutron flux in an environment suitable for placement of a detection system. The research reactor at The Ohio State University Nuclear Reactor Laboratory (OSU-NRL) was the primary location for the experiment because of its known variable flux. This research reactor (OSURR) is a pool-type reactor that is utilized for a variety of instructional, research, and service activities. It is licensed to operate at continuously

variable thermal power up to a maximum of 500 kilowatts, and at maximum steady-state power, the average thermal neutron flux in the core is approximately $5x10^{12}$ n/cm^2/s. The reactor is immersed in a pool of light water that provides moderation and cooling by natural convective flow.[6]

It was assumed the production of a conversion electron in gadolinium will result in a small current pulse height. Therefore, careful consideration was taken when designing the detection system. As with any detection system, noise needed to be reduced. For this experiment, a special high gain, low noise amplifier and pre-amplifier was used. The complete detection set-up is shown in Figure 1-1.

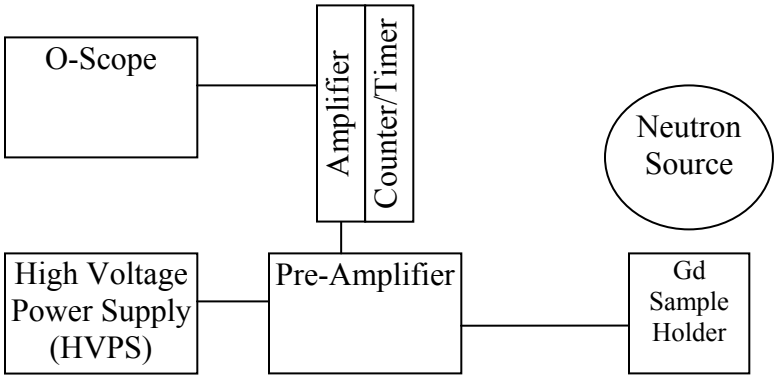

Figure 1-1. Typical detection set-up

After verifying all the components of the detection system functioned properly data was obtained using the OSURR. These measurements were taken with varying fluxes through power variations. The power variations were used to determine that neutrons are being detected. An increase in pulse height with an increase in flux was assumed to be an indication that the pulses were generated by neutrons. The measured leakage current from the IV curves determined the bias required to be applied across the sample.

To fully understand neutron detection in Gd/HfO_2, consideration was taken into the properties this material. Gadolinium doping of hafnium oxide deposited onto a silicon substrate is a new process.[7] Unlike other semiconducting materials, silicon and gallium arsenide for example, the properties are still being studied. Measurements to obtain majority carrier density, carrier mobility, uniformity of deposition, etc were investigated to further understand the usefulness of this material. Microstructure experiments at the LSU synchrotron provided an exploration of the local structure around Gd and the interatomic distances, coordination numbers and Debye-Waller factors for competitive structural models.

1.5. Preview

The Gd L3-edge EXAFS measurements were performed on 3, 10, and 15% Gd doped samples. In all levels of doping, the Gd ion maintains monoclinic local symmetry. The Gd also occupies the substitutional Hf site of the HfO_2 crystalline lattice. Finally, no clustering of Gd atoms was found.[8]

A heterojunction diode composed of Gd doped HfO_2 on silicon has an ability to detect neutrons. The large thermal absorption neutron cross section in Gd is primarily responsible for this result. As these absorptions take place, 72 keV conversion electrons were created and then deposited their total energy in the film. The current pulse generated was measured in a detection system with proper noise reduction. The bias applied to the film was determined to be 0.5 V based on current-voltage measurements.

2. Theory

2.1. Energy bands

Heterojunction diodes are defined by a junction between two semiconductors with differing band gap energies. The separated bands are called valence and conduction, referring to the electron configuration. The former, has its outer shell electrons bound to specific lattice sites within a crystalline structure. The conduction band is a representation of unoccupied electronic states at a temperature equal to absolute zero. The electrical conductivity of a solid is governed by these free electrons. It is helpful to think the conduction band is completely empty and the valence band is completely devoid of electrons. In this configuration, the bands would exhibit no conductivity until enough energy enters material to move an electron across the band gap. Figure 2-1 displays the band structure for an insulator and a semiconductor.

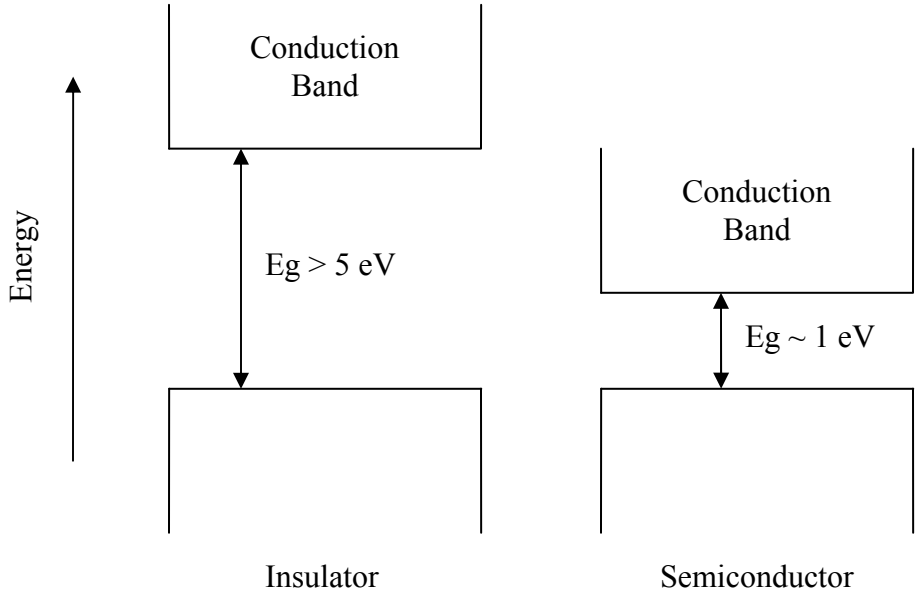

Figure 2-1. Bandgap energies in an insulator and semiconductor

2.2. Charge Carriers

When sufficient energy is applied to a valence electron to move it to the conduction band, two charge carriers are created. These carriers, the electron and the hole left behind, are appropriately called an electron-hole pair. An applied electric field with appropriate voltage can move these charge carriers in opposite directions. This constitutes a current inside the material.

Production of electron-hole pairs through thermal excitation is probabilistically determined and highly dependent on absolute temperature and band gap energy. The relationship is shown in Equation 1.[2]

$$p(T) = CT^{3/2} \exp\left(-\frac{Eg}{2kT}\right) \tag{1}$$

where p(T) is the probability of generation, C is a proportionality constant characteristic of the material, T is absolute temperature, E_g is the band gap energy, and k is the Boltzmann constant.

The exponential terms in Equation 1 show the probability of thermal electron-hole pair generation has a strong negative dependence on a large band gap energy or low temperature. Therefore, an insulator, with its large band gap will have very low conductivity as compared to a semiconductor given equal temperatures. If a pair is created, they will recombine (if an electric field is not present). When the rate of recombination equals the rate of pair generation the material is in thermal equilibrium. When radiation deposits its energy in a material, it will create electron-hole pairs in a local area. These pairs will diffuse throughout the material. Gaussian statistics can be used to predict the distribution of the diffusion of electron-hole pairs throughout a

material. This distribution has a standard deviation as a function of time and the material specific diffusion coefficient. Estimations of the diffusion coefficient and the standard deviation are shown in Equation 2 and Equation 3 respectively.[2]

$$D = \mu \frac{kT}{e} \tag{2}$$

$$\sigma = \sqrt{2Dt} \tag{3}$$

where D is the diffusion coefficient, μ is the charge carrier mobility, k is the Boltzmann constant, T is the absolute temperature, kT/e is the value of 0.0253 eV, σ is the standard deviation, and t is time.

Electron-hole pairs will also undergo a process called drift. This occurs only when an electric field is applied across the semiconductor. The drift velocity is different for the electron than the hole. The hole velocity is generally slower, because for it to move all the electrons must move out of its path. The electron moves opposite the direction of the electric field. The drift velocity is proportional to the electric field and is shown in Equations 4 and 5 for holes and electrons respectively.[2]

$$v_h = \mu_h \varepsilon \tag{4}$$

$$v_e = \mu_e \varepsilon \tag{5}$$

where v_h and v_e are the drift velocities, μ_h and μ_e are the mobilities and ε is the applied electric field.

For small volumes with an applied electric field, diffusion has very little effect on the electron and hole movements. The primary mechanism of movement is the drift velocity. This velocity does reach a value where it no longer increases with an increase

in the applied electric field. This is known as the saturation velocity. Therefore, the movement of the charge carries can be assumed to be at this drift velocity and in the direction of the electric field.

2.3. Dopants and Impurities

In an intrinsic semiconductor the number of holes in the conduction band exactly equals the number of electrons in the valence band. Both electrons and holes contribute to current flow in an intrinsic semiconductor. The amount of current flow is shown in Equation 6.[2]

$$I = \frac{AV}{\rho t} \tag{6}$$

where I is the current, V is the applied bias, ρ is the resistivity, and t is the thickness of the material.

Impurities in a semiconductor are always present even with the best purification processes. However, a material, or dopant, can be intentionally added to vary the electrical characteristics of the semiconductor. A semiconductor is either labeled p-type or n-type based on the dopant material. An n-type material, such as silicon doped with phosphorus, will effectively move the Fermi level towards the conduction band. Since phosphorus has five valence electrons and silicon has only four, the fifth will act as an extra donor. The energy of this donor electron will be in the forbidden region close to the conduction band as shown in Figure 2-2.[2]

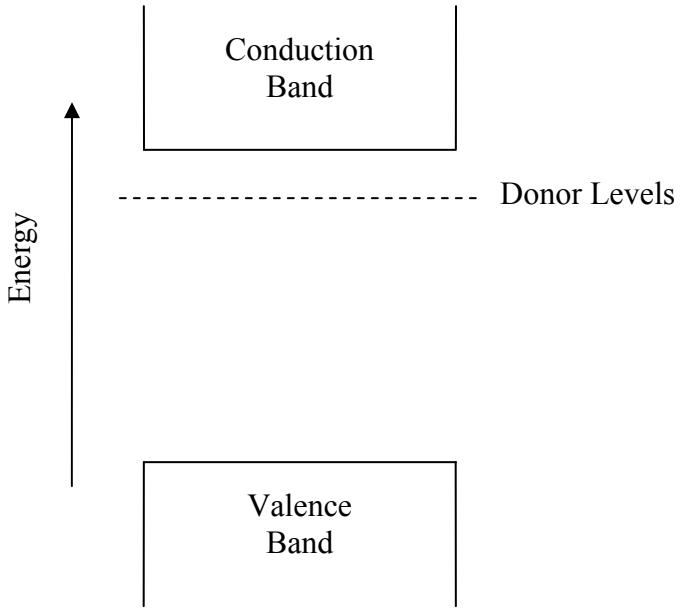

Figure 2-2. New donor levels created with phosphorus in silicon

Conversely, a p-type dopant, such as boron in silicon, will adjust the Fermi level towards the valence band as shown in Figure 2-3. Boron has three valence electrons as opposed to four. It will attract an electron from the valence band and create a hole. This extra hole will capture an electron in the band gap. Although this electron is bound to the boron, it is less tightly bound than it would be to silicon. Therefore, this electron exists in a forbidden energy level and allows easier thermal generation of electron-hole pairs.

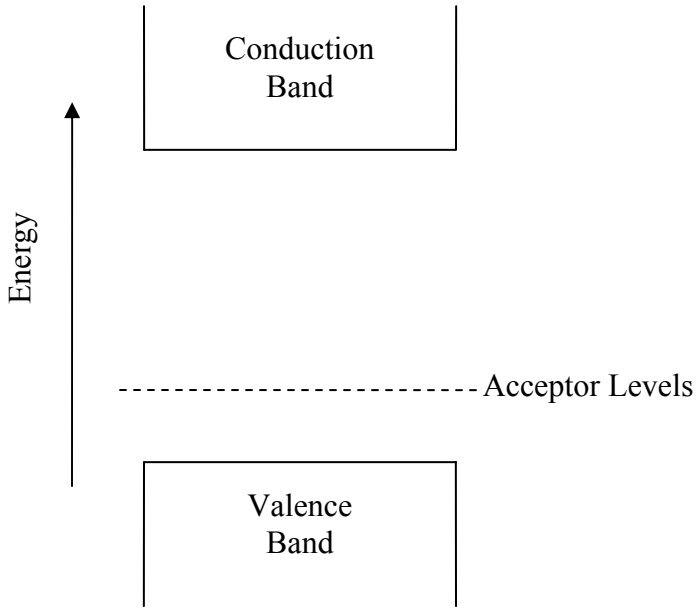

Figure 2-3. Acceptor levels from doping silicon with boron

2.4. p-n and Heterojunction Diodes

A p-n junction is a device used in many applications because it is the building block of many semiconductor devices. These devices are formed when an n-type material is in contact with a p-type material (Figure 2-4). A depletion region is formed at the junction of these two materials. A depletion region is called so because an internal or built-in electric field has swept away all the charge carriers. A heterojunction is formed when to dissimilar semiconductors are joined together. Since the materials are different, they have different band gaps.

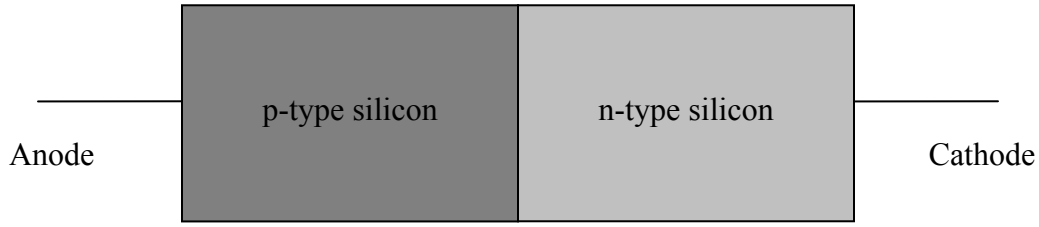

Figure 2-4. A p-n junction

One property that makes a p-n junction useful is its ability to allow current to flow in one direction and not the other (rectification). The area in between the n and p-type regions is a semiconductor with a built-in electric field. This region is non conductive because the electrons in the n-type region recombine with the holes in the p-type region when there is not a sufficient applied electric field to overcome the built-in field. This region can be manipulated to allow electrical flow in either direction by application of a forward or reverse bias.[9]

When a positive bias is applied to the p-type semiconductor material, the diode is said to be in the forward bias condition. The holes in the p-type region and electrons in the n-type region are forced into the depletion region. An increase in forward bias decreases the depletion width, thus limiting the ability of the depletion region to stop carrier motion across it. This allows current flow from the negative to positive ends of the voltage source.

When negative bias is applied to the p-type material, the holes and electrons are pulled away from the depletion region causing it to increase. The widening of the depletion region with increased reverse bias causes a reduction in current flow across the diode. If the electric field is too great, the depletion region breaks down and allows current to flow.

This rectifying property (current flow in only one direction) is the most important characteristic of a p-n junction. A view of current versus bias characteristics illustrates the important features of these junctions (Figure 2-5). When a forward bias is applied, the current rapidly increases with voltage. When reverse bias is applied, the current remains small until a breakdown is reached. At this point, the current increases rapidly.

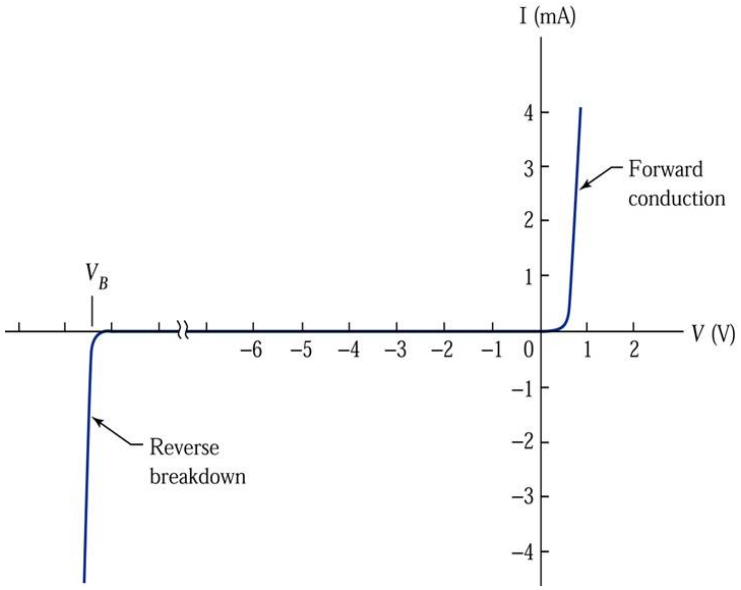

Figure 2-5. Current-voltage characteristics of a typical silicon p-n junction

2.5. Radiation Detection with Semiconductors

A particle entering a semiconductor has a certain probability of interaction based on the semiconductor material and particle type and energy. When an interaction takes place, the energy of the particle is deposited in the medium creating electron-hole pairs within a few picoseconds. With a bias applied across the material, the electron-hole pairs will drift in opposite directions. This movement establishes a current that can be collected until all charge carriers are collected.

Collection of current is only possible with an appropriate type of contact. An ohmic contact is one which permits current flow of any sign (positive or negative). When an electron or hole is created within the detection media, the same type of carrier can be injected into the other side of the diode and the equilibrium concentration can be maintained. At steady state, the use of ohmic contacts, an applied bias, and limited conductivity of a material correspond to a large leakage current causing a significant source of noise. Therefore, great care must be taken to reduce noise in a semiconductor radiation detector.

2.6. Neutron Interaction with Gadolinium

Gadolinium is a rare-earth metal used extensively in the electrical and manufacturing industries. Its extremely large thermal neutron cross section is the reason for its usefulness in the nuclear industry. It has not been widely used in neutron detection because its interaction with neutrons creates fast electrons and gamma rays. Therefore, background gamma radiation causes a more significant problem than a material emitting easier to count heavy charged particles with the employment of pulse shape discrimination methods.

The gadolinium cross section averaged over its naturally abundant isotopes is the largest among all elements (approximately 49000 barns). Gadolinium-157 has the highest isotopic thermal neutron cross section at 255,000 barns and is present in 15.7% of natural Gd. When a Gd atom absorbs a thermal neutron, gamma rays and conversion electrons are created.[5]

The process of ejecting an atomic electron from emitted energy of an excited nucleus is called internal conversion. The ejected electron (typically from the K or L shell) is a competing process with gamma emission. The probability of conversion is the ratio of the number of conversion electrons to that of competing photons. This is known as the conversion coefficient (Equation (7)) and typically increases by Z^3. The kinetic energy of the electron is very close to the excitation energy of the nucleus minus the binding energy of the electron.

$$\alpha = \frac{N_e}{N_\gamma} \tag{7}$$

where α is the conversion coefficient, N_e is the number of conversion electrons, and N_γ is the number of emitted gamma rays.

The conversion efficiency for Gd can reach values of 30-39%. Other efficiencies for elements used in neutron detection such as lithium-6 and boron-10 (low Z) are 1% and 3-4% respectively. Therefore, the emission of the prevalent 72 keV conversion electron in Gd occurs relatively frequently and is an attractive quality for the argument of its use in neutron detection. Also, electrons of this energy have a mean free path of approximately 20 μm in a Gd containing material.[5] Thus, all the electron energy can be deposited in a small semiconducting wafer.

A conversion electron will exert coulomb forces on a large number of atoms while traversing through a material. These interactions are either nuclear or occur between the electron and the atomic electrons of the material. Since the mass of a conversion electron equals the mass of an orbiting electron, it can lose a much larger fraction of its energy versus an electron-nuclear interaction. Both modes of interaction will change the path of

the electron as it travels in a material. These absorptions and reflections are the two methods through which an electron loses energy in a material. Energy imparted to a material will create electron hole pairs. The mean energy for pair production is given in Equation 8.[10]

$$\varepsilon = 2.2E_g + \left(L_i / L_R\right) E_R \tag{8}$$

where ε is the mean energy, E_g is the band gap energy, L_i is ionization mean free path, L_R is the mean free path for scattering with optical phonons, and E_R is the energy of a phonon at the Raman frequency. $(L_i/L_R)E_R$ is estimated graphically in the reference.

2.7. Extended X-Ray Absorption Fine Structure (EXAFS)

Hafnium oxide (HfO_2) is a relatively new material (with respect to its use as a neutron detector) with potential for use as a high-k dielectric oxide.[4] EXAFS is an experimental procedure with the purpose of determining the chemical state and local atomic structure of specific elements.

Information about an element can be obtained by observing emitted photon energy from an excited ion in that element. The impinging x-ray used for excitation must be at a specific energy and based on the material of interest. The energy must equal that of the ionization energy of the core electron to be ejected. These specific energy x rays are produced in synchrotrons and focused through beam lines. After this process, the ejected photoelectron leaves behind a hole and interacts with the surrounding non excited atoms. The wavelength of this electron depends on the energy of the incoming photon. The phase and amplitude of the backscattered wave is dependent on the type of atom and the

distance away from the backscattered atom. This dependence makes it possible for the analysis of EXAFS data to determine structure of the elements of interest.[11]

3. Experimental Procedures

The gadolinium doped hafnium oxide experiments were performed in this research for the purposes of determining material properties and whether the material could be used for detecting neutrons. The process of doping the films was performed without my assistance, so only a short discussion of pulsed laser deposition will be included. The primary experiments discussed here are performing EXAFS, observing current as a function of voltage and temperature, and identifying neutron spectra in a nuclear reactor.

3.1. Pulsed Laser Deposition

Pulsed laser deposition was performed at the University of Nebraska, Lincoln. This process is a physical vapor deposition with the purpose of depositing a material, or dopant, of interest onto a thin film. The technique utilizes a laser focused onto a target in a chamber. The chamber can either be put in a high vacuum or filled with a background gas. The source compound is vaporized and, in turn, deposited onto a supporting substrate.[4]

The Gd-doped films used for experimentation were deposited on single crystal silicon (either p-type or n-type) at a growth rate of approximately 0.15 Å/s. The $GdHfO_2$ source material was prepared using standard ceramic techniques. The materials were powders in the oxide form (HfO_2 and Gd_2O_3). The substrate was cleaned with acid and sputtering and heated to 500 ^{0}C. Pressure inside the chamber was reduced to an initial pressure of 3 x 10^{-7} torr and kept at 10^{-5} torr during deposition. The chamber was also filled with a mixture of helium and argon (8% H_2) to introduce oxygen vacancies.[4] A

simple schematic of this process is shown in Figure 3-1. The area of each sample was assumed to be approximately 0.5 cm x 0.25 cm = 0.125 cm^2. The sample thicknesses (estimated with calipers) were assumed to be approximately 0.0508 cm.

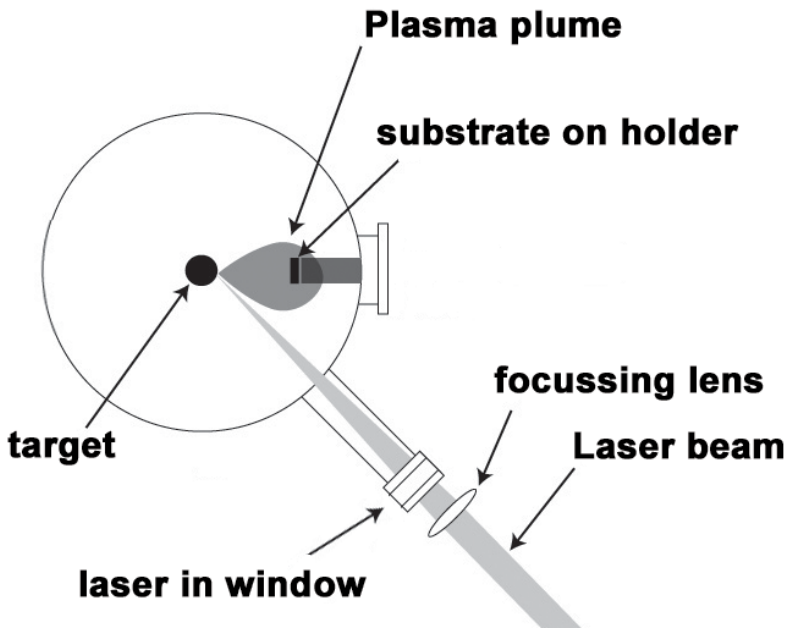

Figure 3-1. Pulsed laser deposition

3.2. Extended X-Ray Absorption Fine Structure (EXAFS)

The experimental procedures for the EXAFS tests were developed by the staff at LSU CAMD facility's synchrotron (Figure 3-2). These consisted of placing the sample into the beam line (Figure 3-3), taking the raw data, and performing data reduction to produce a useable result. Other objectives at CAMD were to observe all these procedures and become familiar with the environment while obtaining this data.

Figure 3-2. Louisiana State University CAMD facility

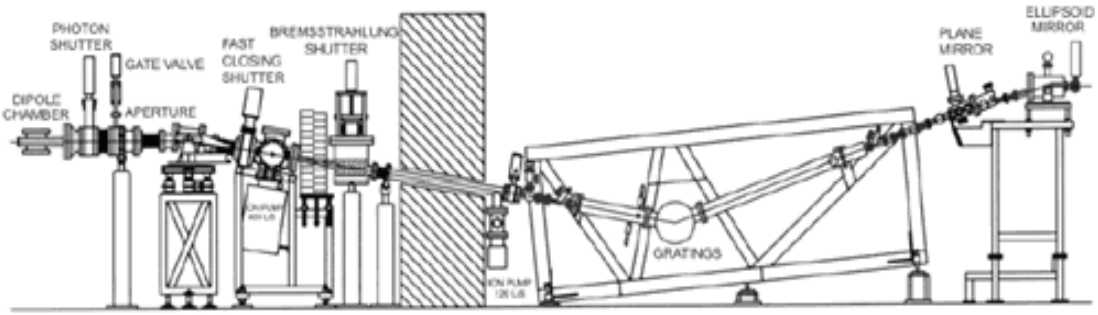

Figure 3-3. CAMD beamline

3.3. Current Voltage Temperature Experiments

A source measurement unit (SMU) coupled with a computer control was used to perform a number of experiments to find the dependence of current on voltage and temperature. These experiments are to ensure proper contact when placing a foil in the sample holder, to observe the shift in the current voltage behavior at various

temperatures, and to identify an appropriate operating voltage to minimize leakage current. The equipment used is listed in Table 3-1 and shown in Figure 3-4.

Table 3-1. TIV equipment

Equipment	Manufacturer	Model
Source Measurement Unit	Keithley	237
Temperature Controller	Lakeshore	331

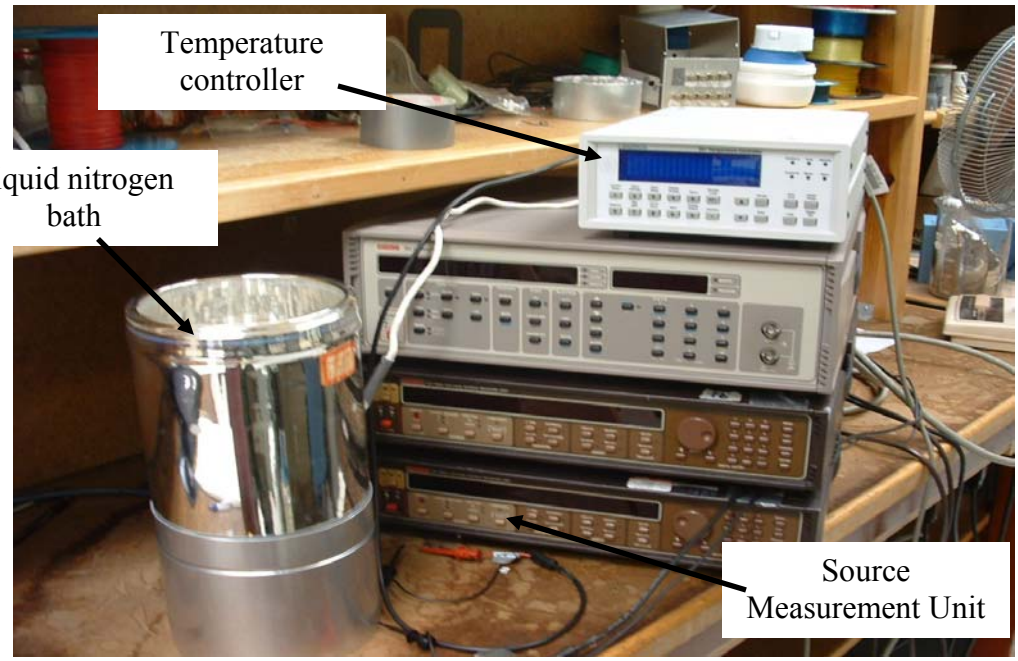

Figure 3-4. Equipment set up

The first experiments were performed to make certain a proper contact can be made between the sample holder and a sample. The sample holder is designed to not only apply a bias and retrieve a generated signal, but also to hold it mechanically in place. Since the samples are fragile, this mechanical contact can cause the samples to crack without warning. The best option for ensuring a contact has been made without damage to the foil was to apply various voltages and measure the currents. When data was

plotted and revealed the expected characteristics, then it can be assumed that an ohmic connection has been made.

A series of these measurements were made on different samples Multiple samples were used because variability existed from sample to sample. Variations were found in doping locations and quality of the contacts. Once these measurements were made, they were plotted and the results compared to the expected IV relationships. The same sample equipment was used to perform temperature dependent measurements with the exception to using a liquid nitrogen bath and temperature controller. The temperature on each foil was varied by immersing the sample holder and foil further in or out of the liquid nitrogen. The temperature controller measured the temperature on the diode. The temperature was allowed to stabilize before measurements were taken.

3.4. Construction of the Sample Holder

An appropriate sample holder needed to be constructed to apply a bias across the diodes and collecting the charges to be sent to the detection system for amplification. Since this holder experiences a high neutron flux it must be made of materials that do not easily activate or capture neutrons.

The holder is shown in Figure 3-5. The major engineering tradeoff in constructing the holder was in substituting materials with high conductivity for materials with a low thermal neutron absorption cross section. For example, building the base plate out of copper would be best for current flow, but would cause major activation problems. These include the neutron reaction with the two natural occurring isotopes of copper (^{63}Cu and ^{64}Cu). Both of these absorb a neutron to create beta particle emitting isotopes.

Therefore, high purity aluminum was selected (T6100 aluminum). An easy choice for the remaining sample holder was Plexiglas. It is easily machined into any shape and its constituents have a low absorption cross section for both fast and thermal neutrons of almost zero.

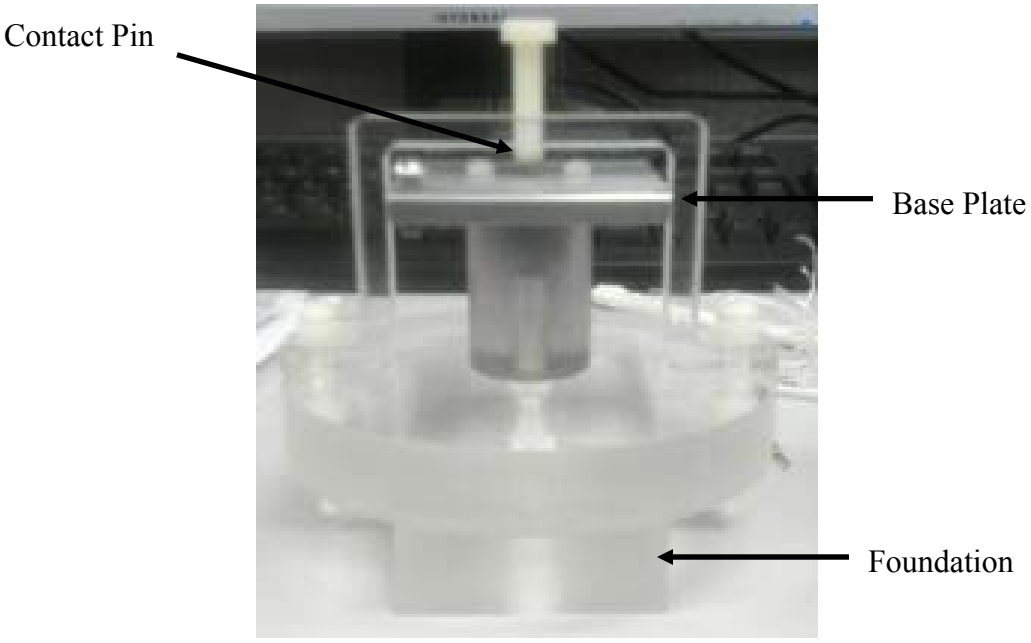

Figure 3-5. Sample holder design

Although copper can easily be activated, it was used as a conductor. The contact pin and wires were both copper, but the mass was small so as to not present much of an activation concern. The major concerns were the hobby box and the BNC connections used to transmit the signals. This box was screwed on over the foundation, acted as a holder for the BNC connectors, and to attach the sample holder into a polyethylene plug for placement into the reactor beam port. A cadmium shell was placed over the box to absorb as many thermal neutrons as possible, so that activation would be minimized. The final sample holder design with polyethylene plug is shown in Figure 3-6.

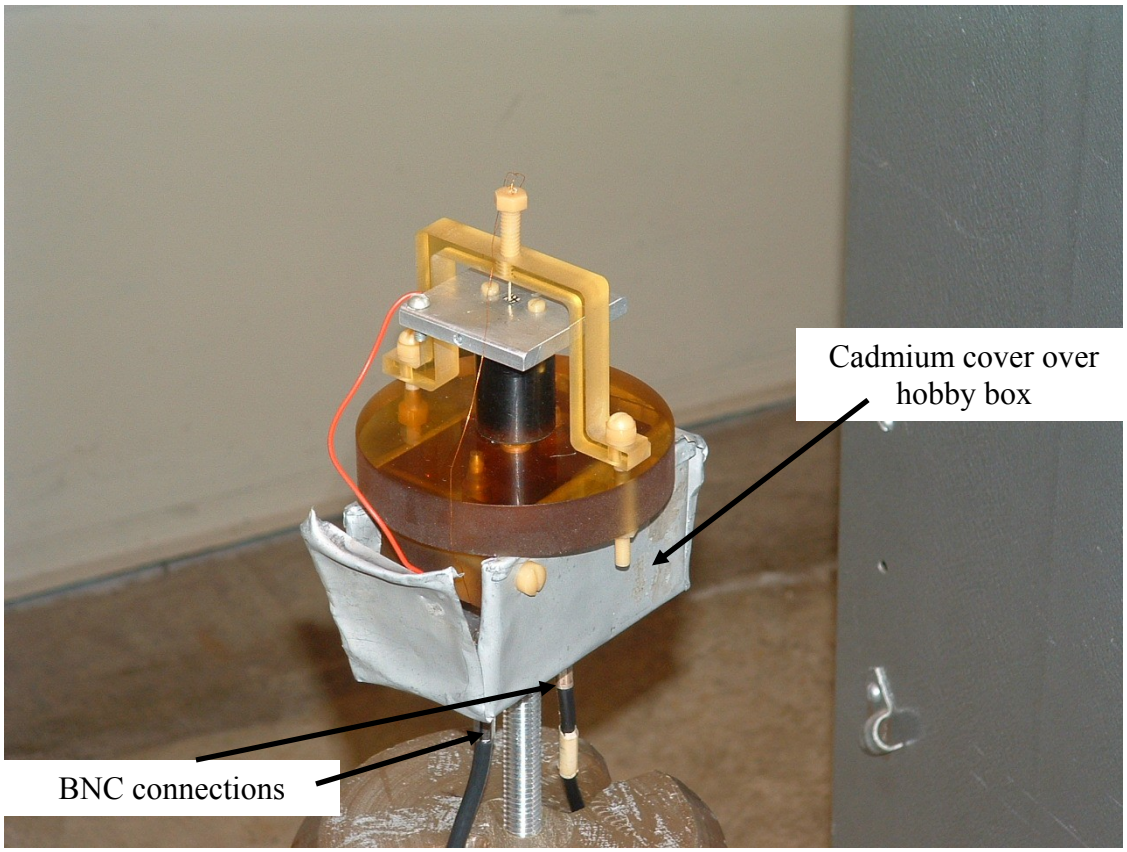

Figure 3-6. Experiment configuration

3.5. Flux Measurements

Foil activation was used to determine the reactor flux as accurately as possible. Total, thermal, and fast flux will be the final determinations in this test. Accurate flux measurements must be made to determine flux in beam port one. The lack of moderator and insertion of the sample holder will cause flux depressions that must be taken into account. The sample holder was placed on the end of the polyethylene plug (Figure 3-7)

and inserted into the beam port (Figure 3-8).

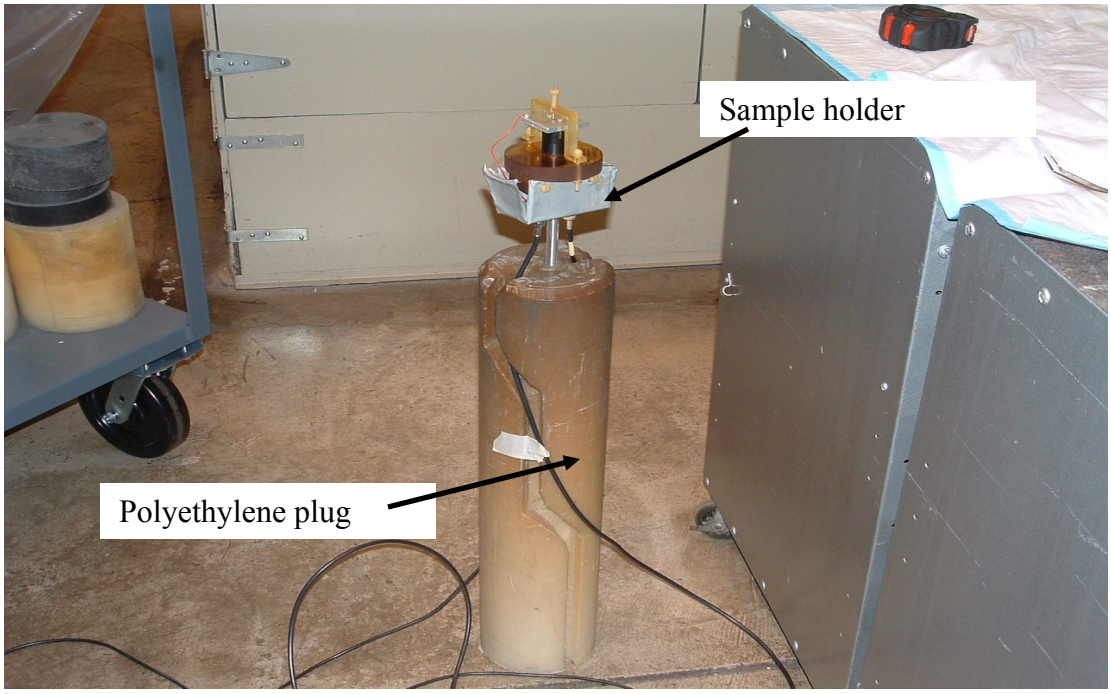

Figure 3-7. Sample holder on polyethylene plug

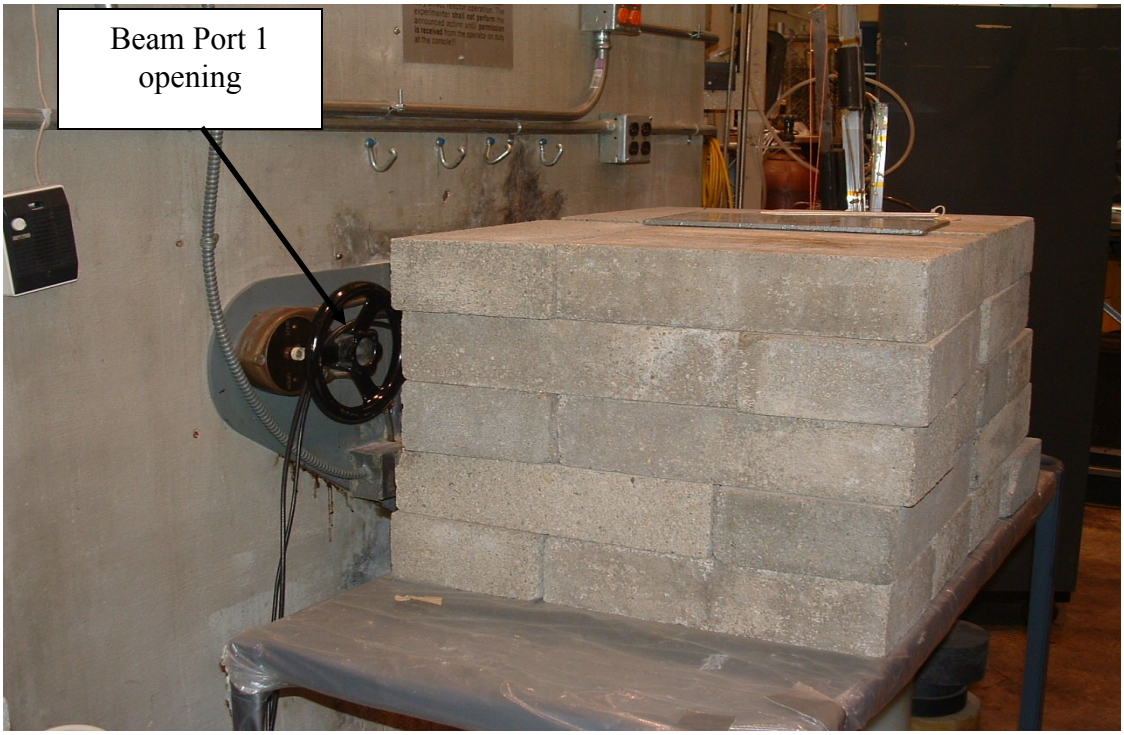

Figure 3-8. Beam port 1

Four dosimeter wires were affixed to the sample holder to simulate the actual testing environment. These dosimeter wires included bare and cadmium-covered copper, gold, and cobalt. The masses of each wire ranged from tens to hundreds of milligrams and were of high purity. The reactor power was set to 10 kW for 30 minutes. Counting of the wires was taken afterwards with a hyper pure germanium counting system on location. The neutron spectrum was estimated using the SAND-II deconvolution code.

3.6. Detection System Set Up and Neutron Detection Experiments

The detection system was designed with the purpose of applying a given bias, accepting the signals created within the foils, amplifying it, and discriminating energies into multiple channels. The equipment used is listed in Table 3-2 and shown in Figure 3-9.

Table 3-2. Neutron detection equipment

Equipment	Manufacturer	Model
ADCAM MCB	Ortec	926
Amplifier	Ortec	572
Counter/Timer	Ortec	996
Pulse Generator	Ortec	419
Oscilloscope	Tektronix	DPO 7104
Preamplifier	Amptek CoolFET	A250CF
Power Supply	Keithley	

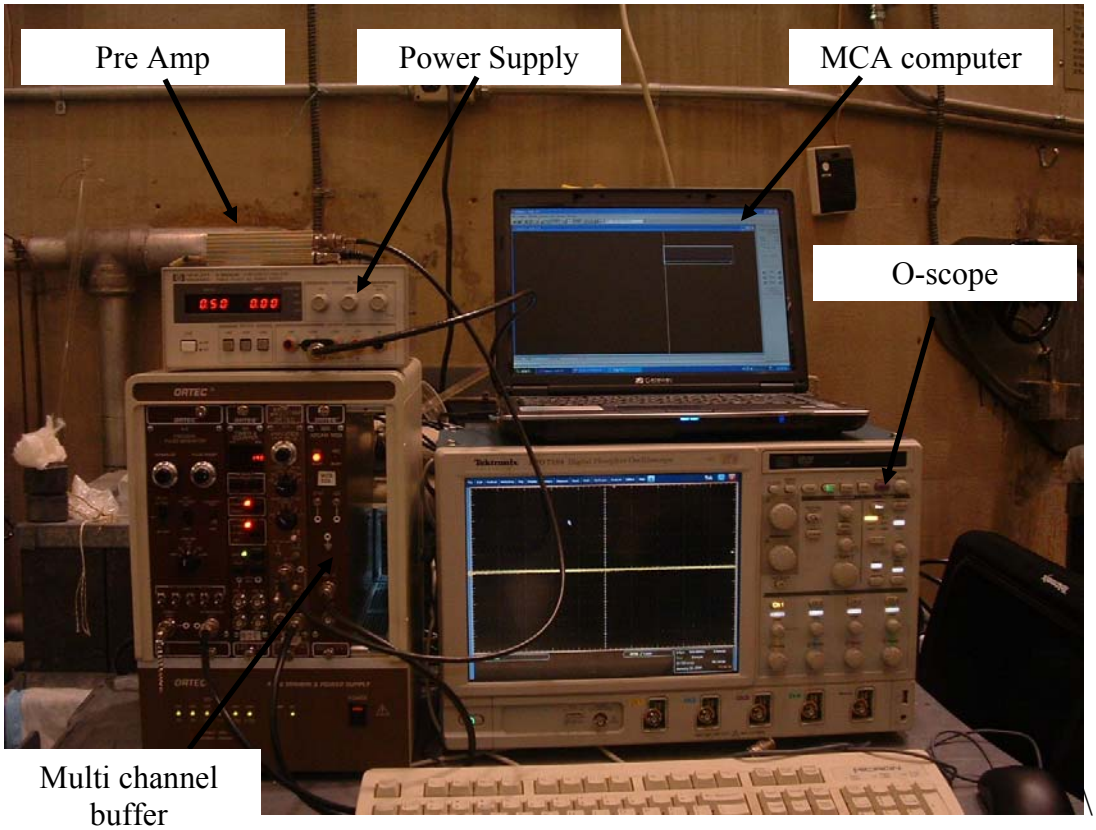

Figure 3-9. Equipment set up

After the equipment was set up and function tested, the sample holder was connected to both the power supply and the pre amplifier. Then the sample holder was screwed into the polyethylene plug as described in the flux measurement section. The sample foil was then held into place between the pin and the base plate to allow current flow. At this point, the plug was inserted into beam port one and ready to take measurements. The voltage was set at 0.5 V (as determined by the current voltage experiment) and set there for the remaining experiments.

A measurement was taken to quantify sources of noise and background inside the beam port. A large amount of noise was detected from the coolant pumps used to provide water flow in the reactor. Three sets of five minute counts were taken to identify

the noise and background. These counts could then be subtracted from the flux measurements to be taken.

Each neutron measurement was taken in sets of three for five minutes (like the background measurements). To ensure the highest probability of observing counts, the first reactor power was set to 450 kW (90% max power). Then the same measurements were taken at 250 kW (50% max power) and 125 kW (25% max power). The idea was to observe a decrease in counts with each power decrease, thus indicating neutron detection.

4. Results and Analysis

4.1. Extended X-Ray Absorption Fine Structure (EXAFS)

The EXAFS experimental results were calculated by the staff at CAMD. Gd L3-edge extended X-ray absorption fine structure (EXAFS) measurements on 3%, 10%, and 15% doped HfO_2 samples were performed using a synchrotron. Figure 4-1 displays the data after Fourier transformation. The peak between approximately 0.8 Å-2.5 Å corresponds to a single scattering contribution from Gd-oxygen pairs. This peak (maximum ~1.7 Å) corresponds to the oxygen coordination number. This indicates the Gd occupies a substitutional Hf site of the $Hf0_2$ crystalline lattice. These data also show there has been no clustering of Gd atoms and the Gd ion retains monoclinic local symmetry for all levels of doping.[8] The peaks at approximately 3 Å and 4Å labeled Gd-Hf+MS and Gd-O+MS in Figure 4-1 are multi-scattering (MS) peaks.

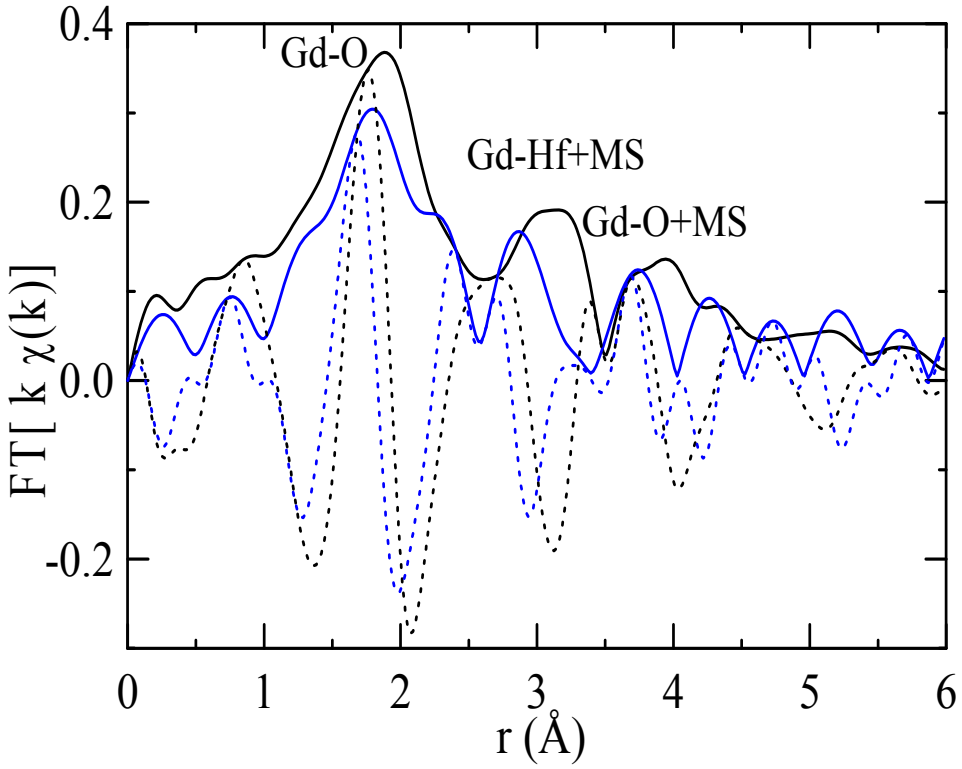

Figure 4-1. Fourier transform plot

4.2. Current Voltage Temperature Experiments

Several I-V measurements were taken with different samples. The first set of samples was much older, and there was evidence of oxidation on the contacts. This was apparent when comparing the reproducibility of the curves. Figure 4-2 is an older sample and Figure 4-3 shows the curve of a sample from the newer set. The SMU applies a constant bias while 64 current measurements are taken. A data point on the plot is an average of those 64 current measurements for each applied bias. After the test had been completed over the entire bias range (between -2.0 to 4.0 volts), the test was reproduced. The reproductions are labeled as trials in the legend of Figure 4-3. The results shown in Figure 4-2 show no reproducibility while each trial for the new sample set shown in Figure 4-3 does. Therefore, only the new set of samples was used for subsequent tests.

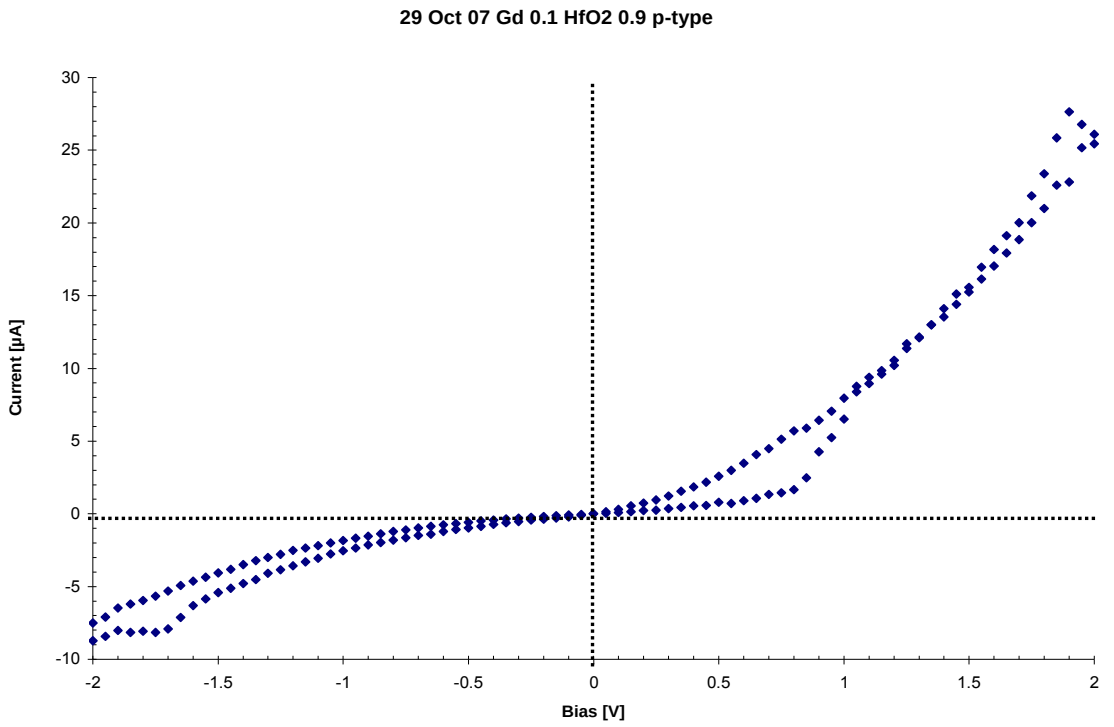

Figure 4-2. Current vs voltage for old sample

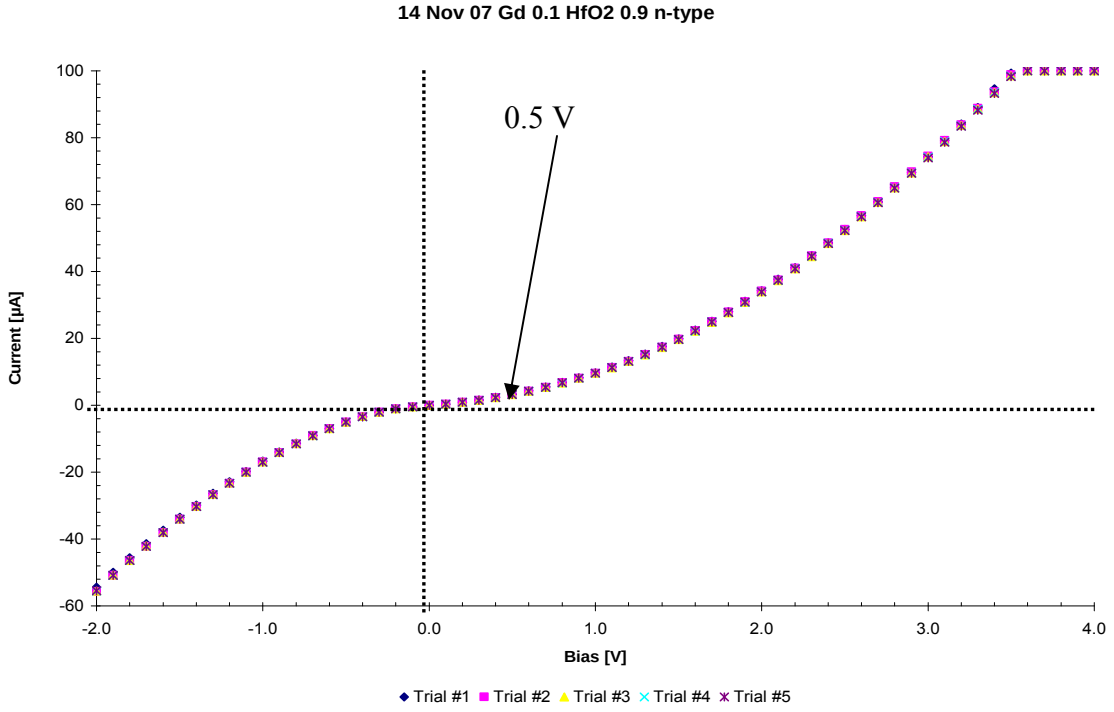

Figure 4-3. Current vs voltage for new sample set

Figure 4-3 shows that the samples do exhibit diode characteristics, however, not of a "good" diode. There is no definite turn-on voltage in the forward bias region and there is a high leakage current. It is the latter of these conditions that is paramount in selecting a bias to apply across the diodes during flux detection experiments. The applied voltage was determined to be 0.5V. This bias was chosen almost arbitrarily because the original idea was to vary the voltage for a series of multiple neutron detection experiments at the reactor. At this voltage (refer to Figure 4-3) the leakage current is relatively low as compared to higher voltages, yet leaves the samples in the reverse bias condition..

Determining dependence of IV curves on temperature was difficult. Each sample cracked or were destroyed when temperatures were below 200K. The responses (shown in Figure 4-4) also yielded results that were not expected. The short (possible) explanation is that the increasing temperature may be increasing defect scattering mechanisms. Scattering mechanisms compete with the increased carrier concentration at higher temperatures. Temperature dependent carrier concentrations are proportional to $T^{3/2}$ while the dependence of carrier mobility due to lattice scattering is related to temperature by $T^{-3/2}$ (both refer to Equation 1 with the same reference). Which property dominates depends on factors such as doping concentration and crystallinity.

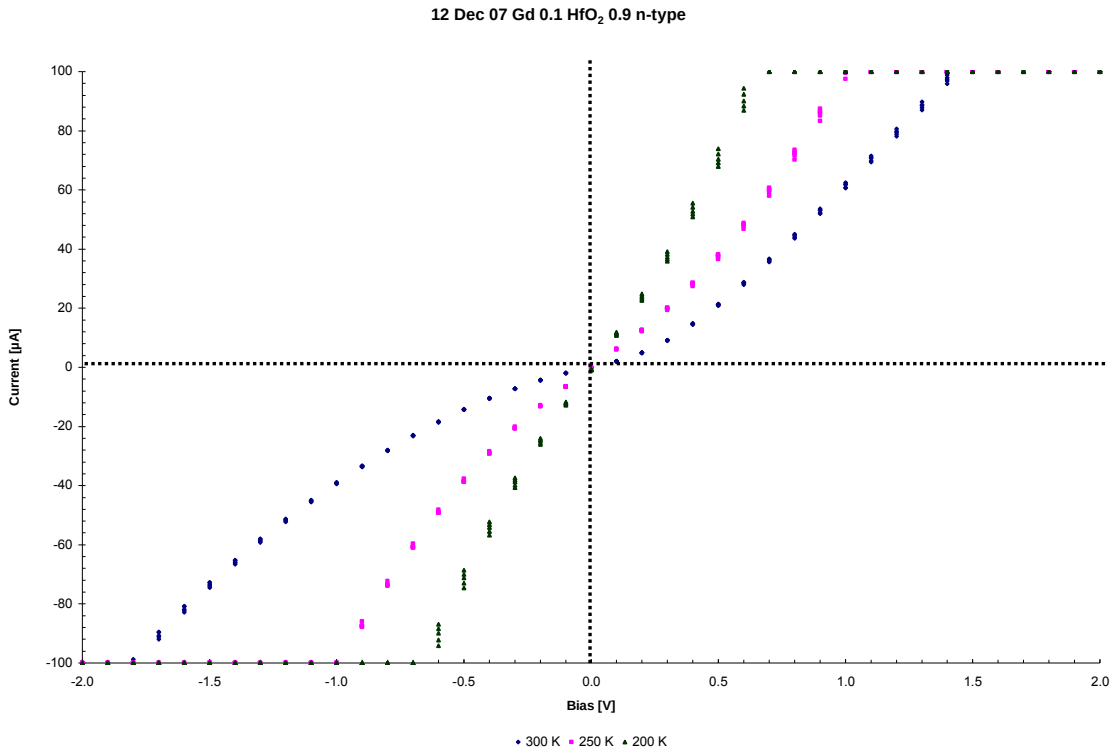

Figure 4-4. Current vs voltage temperature dependence

4.3. Flux Measurements

The fluxes for each power were determined using bare and cadmium covered, high purity copper, gold, and cobalt wires with masses ranging from tens to hundreds of milligrams. These wires were affixed to the sample holder at the same location the semiconductors were placed for testing. After the 30 minute exposure at 10 kW, an overnight decay period was required to reduce the exposure rates from the wire and sample holder activation products. The flux measurements showed results that were expected, meaning the flux values were below the maximum reactor flux of 3×10^{13} n/cm^2-s. Lower flux values were expected because the sample location will not be in the reactor core and the holder is in place of moderating material usually in place. The total

thermal fluxes for 450 kW, 250 kW, and 125 kW were 2.57 x 10^{12} n/cm^2-s, 1.48 x 10^{12} n/cm^2-s, and 7.14 x 10^{11} n/cm^2-s respectively. The results for each flux measurement and deconvolution are shown in Figure 4-5. Each of these fluxes will be used to determine efficiencies in the neutron detection experiments.

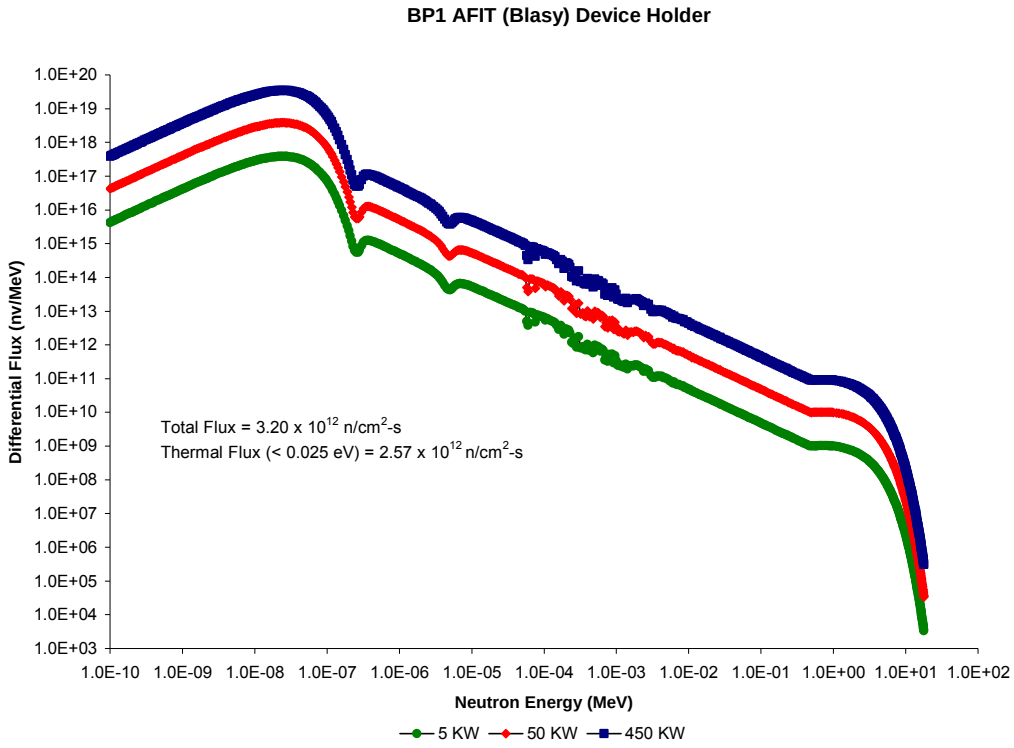

Figure 4-5. OSU flux spectra

4.4. Neutron Detection Experiments

The measurement of 72 keV electrons from neutron interactions is not immediately apparent during irradiation in the reactor. This is due to background counts and noise from the coolant pump. The background spectrum is shown in Figure 4-6.

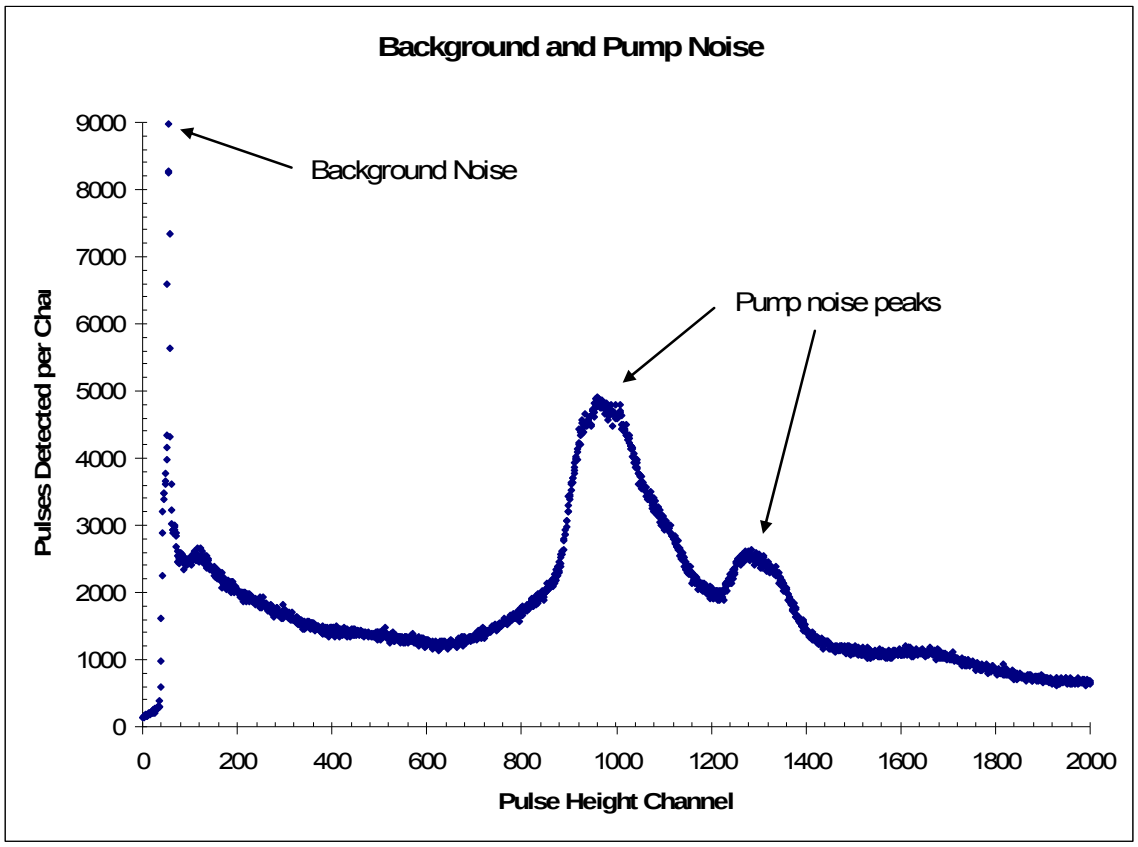

Figure 4-6. Background and pump noise

The background and pump counts were subtracted from the counts taken during the neutron detection experiment spectra. The background counts in each channel were subtracted from the same channel in the gross count spectra. Once the background counts were subtracted from the total spectra taken at each power level, energy peaks were observed. These are shown in Figure 4-7, Figure 4-8, Figure 4-9, and Figure 4-10.

Two peaks were observed for each power level. The first was the desired 72 keV conversion electron peak and the second was a 79.51 keV gamma peak from the (n,γ) reaction. The 72 keV electrons only require 72 microns of material to deposit all of their energy and the 79.51 keV photons require approximately 3100 microns. Therefore, less energy is deposited in the film resulting in a better resolution for the 72 keV electron

peak. Photons of higher energies are also emitted when gadolinium absorbs a neutron. The next highest is a 182 keV photon emitted 100% of the time, but this requires approximately 67 cm for 99% of the energy to be deposited and 1.5 cm to capture only 10% of the energy. Therefore, this photon or any photons with higher energies were not observed in the spectrum.

The full energy peaks were identified in relatively low channels (channel 38 for 72 keV and 78 for 79.5 keV). Since the detection system is not calibrated, the expected channel was estimated for verification. Voltage equals charge divided by capacitance. Dividing the 72 keV conversion electron energy by the value for the mean energy for an electron-hole pair (using the Shockley equation) will estimate the charge. The Shockley equation (Equation 8), gives a value of 14.5 eV. This results in a charge of 1.59×10^{-15} C (must multiply by 2 because of both electrons and holes). The capacitance of the CoolFET pre-amplifier equals 0.5×10^{-12} F. Assuming a ratio of 1024 channels over 10 V for the multi channel analyzer and an amplifier gain of 14 (20 coarse gain multiplied by 0.7 fine gain) these calculations give an estimated channel of 9. This was used for order of magnitude estimation only and gave an indication that the peaks should be identified in low channels.

One important observation is the number of counts increased in each peak as the flux increased. Although only one bias was able to be applied to the films, this indicates neutron detection had occurred. A negative aspect of using this material for detection is the terribly low efficiency. These absolute efficiencies were calculated by dividing the number of counts below each full energy peak by the number of neutrons incident in the sample medium. The greatest efficiency was 1.36×10^{-11} at 450 kW.

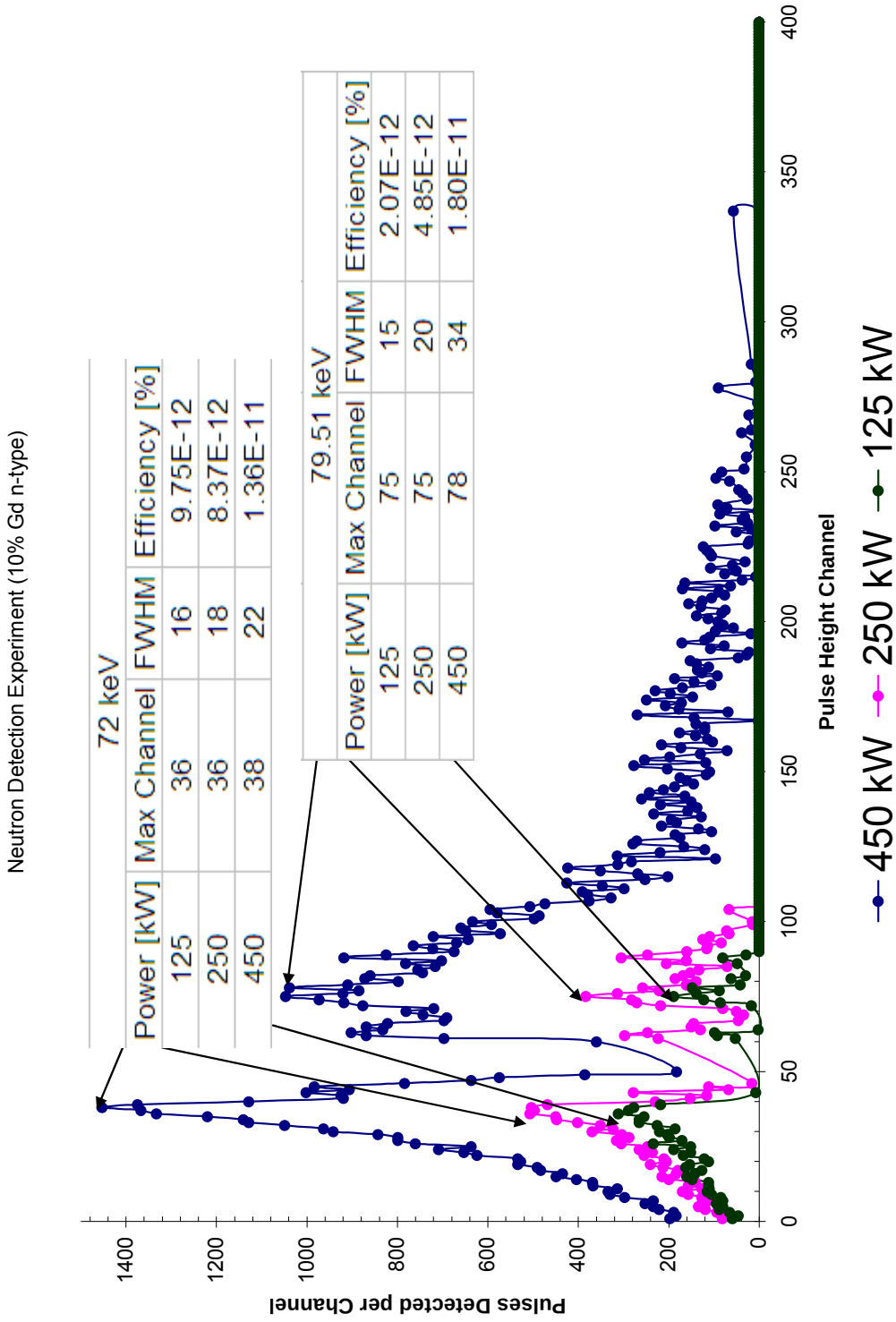

Figure 4-7. Neutron spectra power comparison

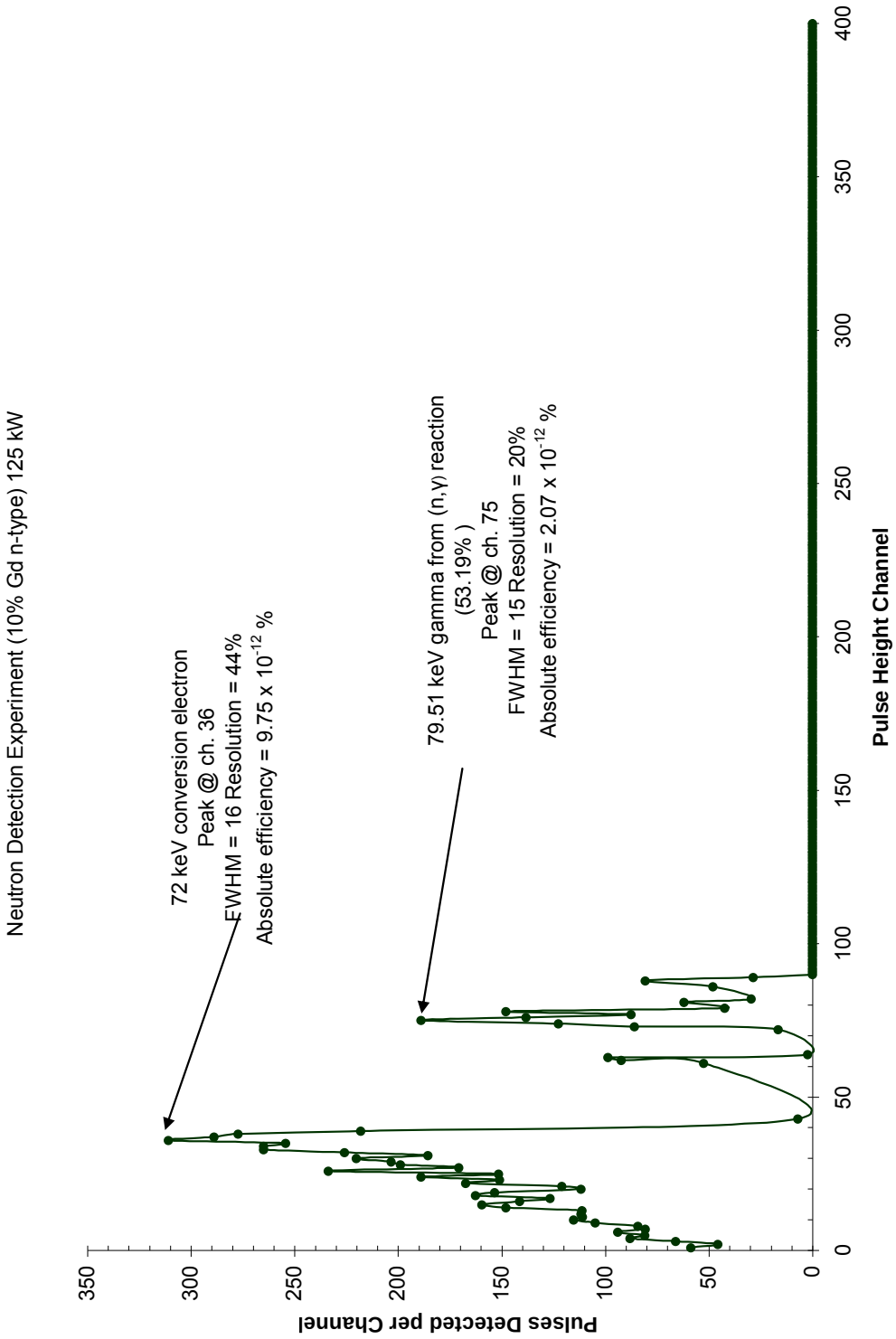

Figure 4-8. 125 kW neutron spectrum

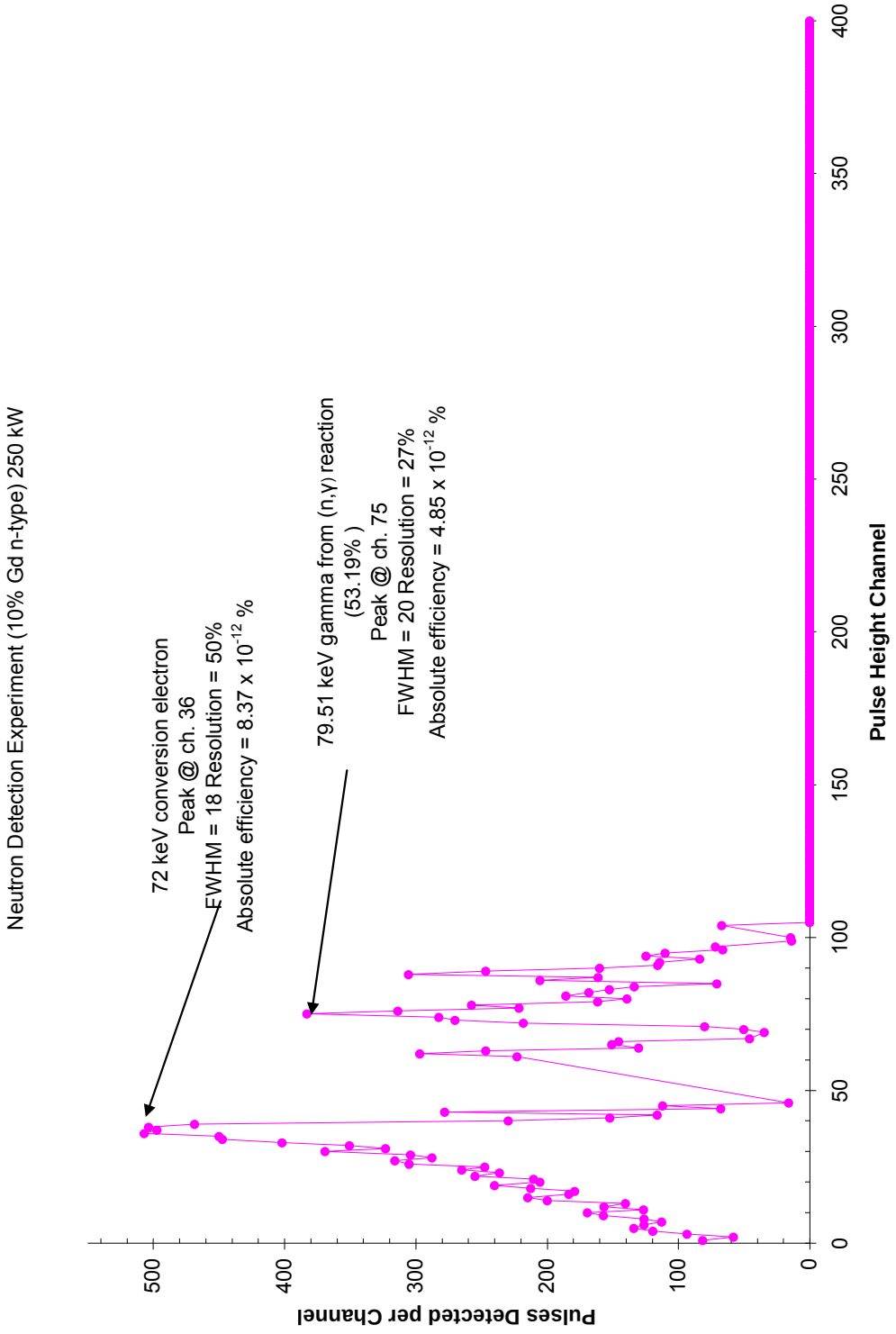

Figure 4-9. 250 kW neutron spectrum

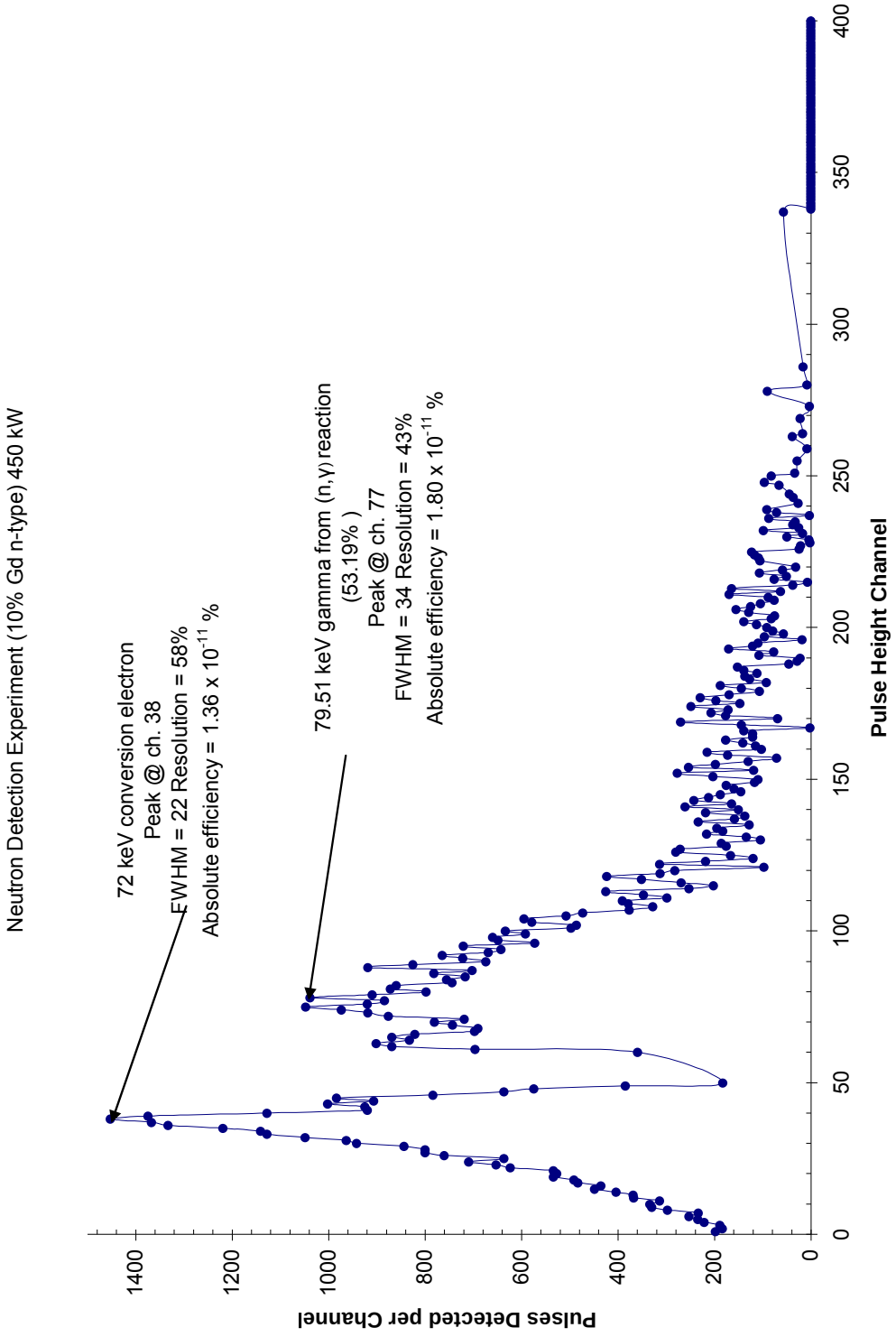

Figure 4-10. 450 kW neutron spectrum

5. Conclusions and Recommendations

As with many experiments, more research in the areas investigated in this thesis is possible. Due to limited time and resources, these could not be completed. This chapter briefly discusses a few of these.

The IV-T experiments yielded results that were not expected. These should be repeated with more samples, however, the samples are so fragile, new, and more durable wafers must be produced. Every sample shattered when reaching approximately 200 K during these experiments.

An expansion to the neutron detection experiment would include increasing the bias across the diode. A voltage increase would move the counts into channels further outside of noise and could increase the extremely low detection efficiency if there is complete charge collection. However, there is a tradeoff because leakage current will be increased at these higher voltages. An experiment showing the effect of bias should be done between zero volts and some high voltage to accurately show the effect of neutron detection on applied bias.

One of the major problems with obtaining good data in all of the experiments was the sample holder. Although it adequately allowed the sample to function as a detection medium, the sample was held in place with a mechanical contact. The copper pin came from the top of the holder and was held firmly to a sample by screwing it down tighter. This also turned the pin while resting on the contact and resulted in scratching it off. It was also very difficult to assess how much pressure was put on the delicate wafers. Some would crack if little care was taken. A new design should incorporate a spring

mechanism so the pin will move when applying pressure. Another observation was that the Plexiglas melted after irradiation at approximately 16 hours of being inside the OSU reactor at 90% power. If this same design is to be used, an approximation of how long it will last can be made by the color change in the Plexiglas. After the flux experiment, around 10% power for approximately 30 min, it changed slightly yellow. The next experiment was operating the reactor at 90% power for about 6 hours. The color change after this test was very apparent. The sample holder broke during the last experiment when trying to vary voltage at 90% power.

Gd doped HfO_2 was able to be used in a detection system and displayed the ability to detect neutrons. If future research is done with this material, observations could be made pertaining to bias changes; however these should be completed using better samples. Employing a detection system with this material is years in the future even if great strides can be taken in forming better diodes and increasing detection efficiency.

6. Bibliography

1. http://www.dtra.mil/index.cfm

2. Knoll, Glenn F. *Radiation Detection and Measurement (3rd Edition).*11:353-360 New York: John Wiley & Sons, 2000

3. Baum, Edward M and others. Nuclides and Isotopes Chart of the Nuclides (16th Edition). KAPL, Inc, 2002

4. Dowben, P. A. and others. *The n-Type Gd-Doped HfO_2 to Silicon Heterojunction Diode*, 6 April 2007. Lincoln, Nebraska: Department of Physics and Astronomy and the Nebraska Center for Materials and Nanoscience, University of Nebraska-Lincoln

5. Knoll, Glenn F. *Radiation Detection and Measurement (3rd Edition).*14:509 New York: John Wiley & Sons, 2000

6. http://www-nrl.eng.ohio-state.edu/

7. Debernardi, A. and Fanciulli, M. *Structuarl and Vibrational Properties of High-Dielectric Oxides, HfO_2 and TiO_2: A Comparative Study*, 22 November 2006. Agrate Brianza, Italy: MDM National Laboratory

8. Ignatov, A. U. and others, *The Location of the Gd atom in Gd-doped HfO_2*, 2007, Lincoln, Nebraska: Department of Physics and Astronomy and the Nebraska Center for Materials and Nanoscience, University of Nebraska-Lincoln

9. Sze, S.M. Semicondutor Devices Physics and Technology (2nd Edition). New York: John Wiley & Sons, 2002

10. Buaaolati, C. and Piorentini, A. *Energy for Electron-Hole Pair Generation in Silicon by Electrons and α Particles*, 27 July 1964, Milano, Italy: Laboratori CISE

11. Newville, Matthew, *Fundamentals of XAFS*, 23 July 2004, Chicago, IL: Consortium for Advanced Radiation Sources, University of Chicago

REPORT DOCUMENTATION PAGE

Form Approved
OMB No. 0704-0188

PLEASE DO NOT RETURN YOUR FORM TO THE ABOVE ORGANIZATION.

1. REPORT DATE *(DD-MM-YYYY)*	2. REPORT TYPE	3. DATES COVERED *(From - To)*
27-03-2008	Master's Thesis	June 2007 - March 2008

4. TITLE AND SUBTITLE

Neutron Detection Utilizing Gadolinium Doped Hafnium Oxide Films

5a. CONTRACT NUMBER

5b. GRANT NUMBER

5c. PROGRAM ELEMENT NUMBER

6. AUTHOR(S)

Blasy, Bryan D., 2Lt, USAF

5d. PROJECT NUMBER

JON 08-318

5e. TASK NUMBER

5f. WORK UNIT NUMBER

7. PERFORMING ORGANIZATION NAME(S) AND ADDRESS(ES)

Air Force Institute of Technology
Graduate School of Engineering and Management (AFIT/EN)
2950 Hobson Way, WPAFB OH 45433-7765

8. PERFORMING ORGANIZATION REPORT NUMBER

AFIT/GNE/ENP/08-M02

9. SPONSORING/MONITORING AGENCY NAME(S) AND ADDRESS(ES)

1Lt Aaron L. Arting
AFRL/RDHP, Bldg 324
3550 Aberdeen Ave SE
Kirtland AFB NM 87117

10. SPONSOR/MONITOR'S ACRONYM(S)

11. SPONSOR/MONITOR'S REPORT NUMBER(S)

12. DISTRIBUTION/AVAILABILITY STATEMENT

APPROVED FOR PUBLIC RELEASE; DISTRIBUTION UNLIMITED

13. SUPPLEMENTARY NOTES

14. ABSTRACT

Gadolinium (Gd) doped hafnium oxide (HfO_2) was deposited onto a silicon substrate using pulsed laser deposition. Synchrotron radiation was used to perform Gd L3-edge extended X-ray absorption fine structure (EXAFS) measurements on 3%, 10%, and 15% doped HfO_2 samples. The interatomic distances determined from Fourier transformation and fitting the data show Gd occupying the hafnium site in the HfO_2 lattice, there was no clustering of Gd atoms, and the Gd ion retains monoclinic local symmetery for all levels of doping. Current as a function of voltage experiments identified the films as having poor diode characteristics with high leakage current in the forward bias region. However, a proper bias (0.5 V) for the purpose of neutron detection was identified and applied across the diodes. Using a high, non-varying neutron flux in a nuclear reactor, Gd doped HfO_2 was able to be used in a detection system and displayed the ability to detect neutrons.

15. SUBJECT TERMS

Gadolinium, Radiation, Neutron, Semiconductor, Hafnium Oxide

16. SECURITY CLASSIFICATION OF:			17. LIMITATION OF ABSTRACT	18. NUMBER OF PAGES	19a. NAME OF RESPONSIBLE PERSON
a. REPORT	b. ABSTRACT	c. THIS PAGE			David A. LaGraffe, LTC, AFIT/ENP
U	U	U	UU	59	19b. TELEPHONE NUMBER *(Include area code)* (937)255-3636 x-7308 david.lagraffe@afit.edu

Reset

Standard Form 298 (Rev. 8/98)
Prescribed by ANSI Std. Z39.18